Functional enzymatic assays to predict the potency of extracellular vesicles

Giorgia Adamo,[*a] Sabrina Picciotto,[a] Paola Gargano,[a] Angela Paterna,[b] Estella Rao,[b] Samuele Raccosta,[b] Monica Salamone,[a] Daniele Paolo Romancino,[a] Mauro Manno,[b] and Antonella Bongiovanni.[*a]

a.Cell-Tech HUB and Institute for Research and Biomedical Innovation, National Research Council of Italy (CNR), Palermo 90146, Italy. **b**. Cell-Tech HUB and Institute of Biophysics (IBF) CNR, Via Ugo La Malfa 153, 90146 Palermo, Italy.

*giorgia.adamo@irib.cnr.it;
*antonella.bongiovanni@irib.cnr.it.

The establishment of an extracellular vesicle (EV) functional assay is essential for defining the bioactivity, quality, batch-to-batch reproducibility and stability of EV preparations to facilitate subsequent applications as therapeutics or carriers for cell-free therapies. The high heterogeneity of EV preparations requires a sensitive test that supports gold-standard-methods reported in the Minimal Information for Studies of Extracellular Vesicles (MISEV, 2018) guidelines for the functional characterization of EVs. Here, we developed a ubiquitous enzymatic-based assay for EVs, a single-step functional analysis to predict their potency that simultaneously allows a quantitative measure of EV-bioactivity and vesicle integrity, using small-size EV samples. In particular, we set up and validated this robust and simple test using nanoalgosomes as EV-model system, selecting a specific substrate for enzymes present the vesicular cargo of several type of EVs, including mammalian's one. We also explored the proposed assay's potential for EV-quality check after different EV-isolation, storage, and loading methods.

Keywords: extracellular vesicles, integrity, bioactivity, functional enzymatic assay, potency, quality, standardization

Introduction

Extracellular vesicles (EVs) are essential signaling mediators that are involved in intercellular and inter-organism communications.[1,2] EV signals depend on their cargo, which can be naturally-sourced bioactive molecules such as proteins and nucleic acids, or exogenously loaded (e.g., RNAs or drugs).[3,4]

In recent years, EVs have come to be considered one of the most promising bio-nanovehicles in cell-free therapies.[5] However, despite the advances in the field, many challenges with EV-based therapies remain, such as the non-scalability of the EV production process, the still inefficient EV payload uptake, the need to optimize tropism and biodistribution while minimizing adverse effects.[6] The therapeutic efficacy of EVs depends on a variety of additional parameters, some of which can be addressed only during laborious and expensive preclinical trials.[7] To validate the quality of EV preparations and define the Critical Quality Attributes (CQA), EV-inherent features should be tested to qualify them as suitable for subsequent clinical functional testing applications.[8]

Ideally, specific functional assays would predict whether a particular EV-preparation holds the potential to achieve its intended therapeutic effects, which could be further investigated in a "formal disease-specific" functional assays.[7,9]

The MISEV-2018 guidelines propose rigorous procedures required to document specific EV-associated functional activities to cope with the advance of EV research, assuring and improving the quality of these studies.[10]

In this view, to achieve an adequate assessment of EV bioactivity, appropriate functional assays need to be created to support common EV-related biophysical and biochemical quality controls (QCs) and to specifically predict EV potency. Furthermore, a functional assay should be simple and sensitive enough using low amount of EV samples to facilitate the following functional studies.[11,12] To date, many in vitro and in vivo assays have been used to interrogate the potency of specific types of EVs; however, many of them failed for several challenges that make reliable assays difficult to set up.[7,13] In the field of extracellular vesicles, it is expected that no single test can adequately measures all product attributes that predict clinical efficacy. The development of ubiquitous, standardizable and functional test for evaluating the bioactivity can be tricky for extracellular vesicles because they are highly heterogeneous and show different functional activities.[14] Despite this evidence, there is a need for a precise procedure to accurately determine the bioactivity and identity of EV preparations, which can be applied to various types of EVs, regardless of their origin or preparation method.[12]

In this study, we proposed a new, simple, highly sensitive and precise functional assay to predict the potency of EVs by contextually evaluating the enzymatic activity and membrane integrity, using a fluorescein diacetate-based enzymatic method.[15,16]

Results and discussion

Beyond fluorescein diacetate based-method for EVs

Fluorescein diacetate (*i.e.* 3'-6'-diacetyl-fluorescein, FDA) is a non-fluorescent fluorescein molecule conjugated to two acetate radicals. This is a fluorogenic ester compound able to pass through phospholipid bilayers like plasma and EV membranes. Indeed, when inside cells or EVs, FDA is hydrolyzed by non-specific esterases to produce a negatively charged membrane-impermeable green fluorescent molecule (i.e., fluorescein).[17] This membrane-permeable esterase substrate can be used both to measure enzymatic activity, which is required to activate its fluorescence, and to evaluate membrane integrity, which is necessary for the intracellular or intra-vesicular retention of its fluorescent product **(Figure1).**

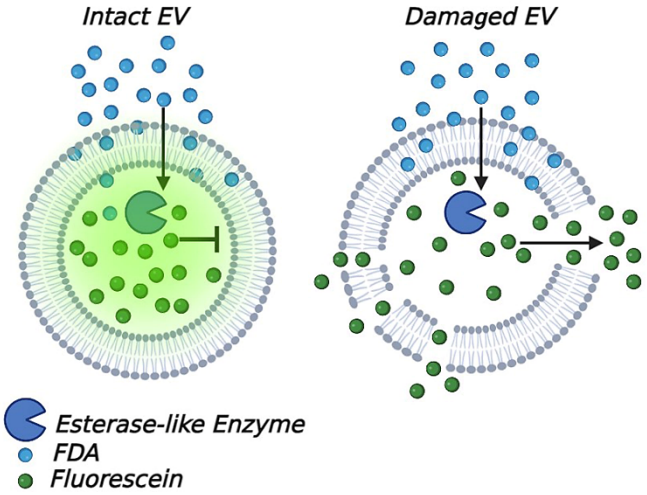

Figure 1. Graphic representation of fluorescein diacetate behaviour in intact and damaged EV.

FDA is commonly used as a probe to study microbial metabolic activity or to monitor the cell viability of fungi, plants, microalgae, and bacteria, giving information both on enzymatic activity and cell integrity which is mandatory for intracellular detection of its fluorescence.[18,19,20,21] In the EV-field, different approaches have described the use of membrane-permeant enzyme substrates to label EVs, including carboxyfluorescein diacetate-acetoxymethyl ester (CFDA), carboxyfluorescein diacetate succinimidyl ester (CFSE), and calcein acetoxymethyl ester (calcein-AM).[18,22,23,24] Similarly to FDA, these molecules are cleaved by enzymes which are present inside cells as well as in secreted EVs. These experimental approaches have been developed to make EV fluorescent and detectable for flow cytometry applications or for fluorescent microscopy; so these methods are not quantitative and do not directly provide information on EV-functional activity and quality.[25] Beside, an important aspect to be considered during the development of an EV-based functional assay is to identify a common key feature which is also quantifiable, standardizable, and suitable for EVs isolated from different sources. An analysis of the publicly available *ExoCarta* database (http://www.exocarta.org) showed a noticeable and extremely robust association between esterase-like enzymes as EV-cargo components and EVs derived from many mammalian sources (mice, rats, and cows), including several body fluids (blood, saliva, and urine) and several human cancer and normal cells (more than 60 hits for "esterase" from the ExoCarta database).[26,27] Furthermore, many recent proteomic analyses described the presence of esterase-like enzymes in EVs isolated from bacteria (like *Escherichia coli* and *Pseudomonas aeruginosa*), plants and fungi (*Candida albicans* and *Aspergillus fumigatus)*.[28,29,30,31,32,33] Taking all these considerations into account, we developed an FDA-based method with a reliable and quantifiable read out for the enzymatic activity in EVs **(Figure 2)**. First, we checked whether we could measure a time-dependent fluorescence signal by incubating small volumes of extracellular vesicle samples with the FDA substrate, which could be detected by spectrofluorimetric measurements. For this purpose, we used microalgae -derived extracellular vesicles (called nanoalgosomes or algosomes) as EV models. After we found that nanoalgosomes contain active enzymes such as esterases, we established the experimental conditions necessary to develop a functional assay.

Throughout this process, we considered various aspects crucial for working with EVs to predict their potency. For example, we applied the functional assay to compare the quality of different EV batches or EVs isolated using different methods (such as differential ultracentrifugation versus tangential flow filtration). Additionally, we assessed the bioactivity and integrity of EVs stored under different conditions or manipulated using various physical loading techniques, using the proposed functional test and comparing these results with the ones of standard methods for EV evaluations, such as nanoparticle tracking analysis or bicinchoninic acid assay.[10] The results encouraged the application of the functional enzymatic assay, here proposed, for rapid QC check of EVs, as in a single step analysis giving two important pieces of information: the bioactivity and the membrane integrity of EV preparations.

Proof of concept: fluorescein diacetate based-assay to test nanoalgosome bioactivity

To explore the bioactivity of nanoalgosomes, we started by evaluating the presence of active enzymes, like esterases, which are able to convert the FDA substrate into fluorescent fluorescein. FDA was one of the first membrane-permeant fluorescent probes used to study cell viability in a wide range of systems, such as mammalian cells, microalgal cells, fungi, plant cell cultures, and protoplasts.[34] FDA is permeable to membranes in its native state, and after entering a living cell or membranous

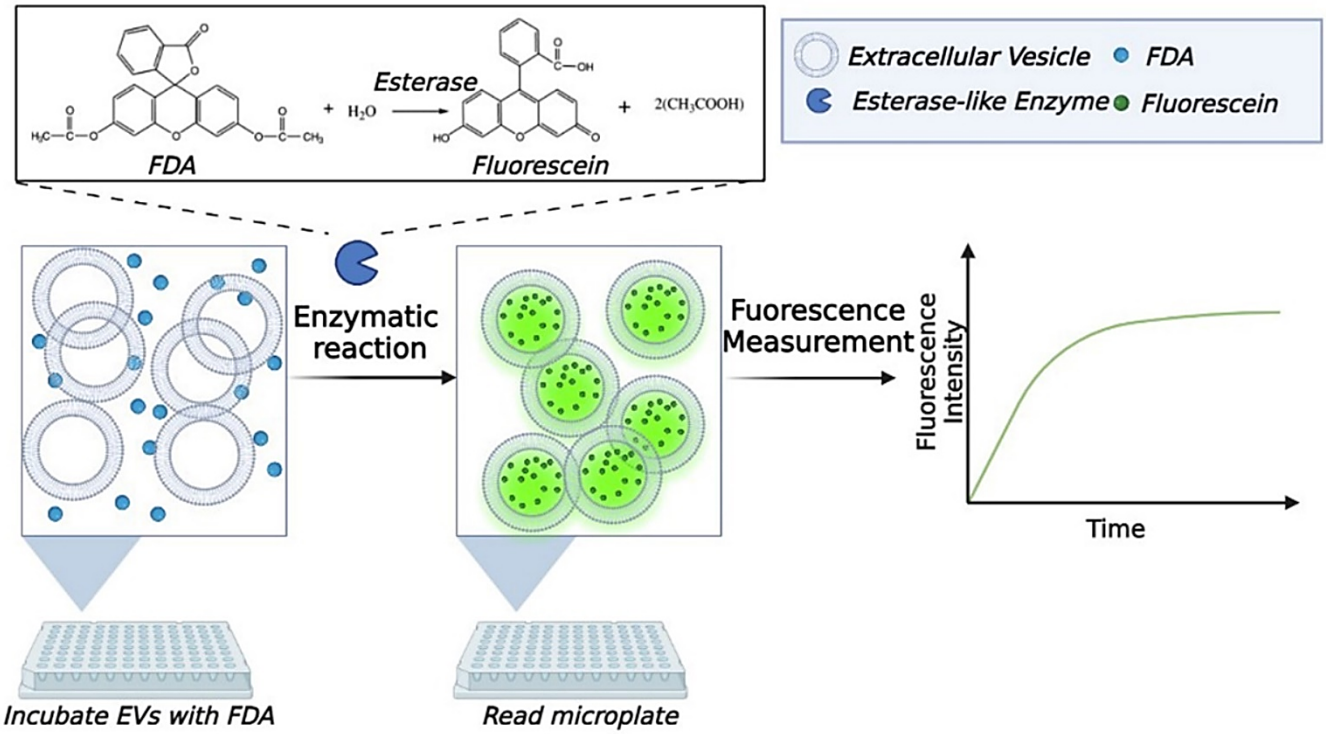

Figure 2. Schematic representation of the strategy applied for the development of a functional enzymatic assay for extracellular vesicles.

structures, the acetate moieties could be enzymatically cleaved, producing fluorescein, which is membrane impermeable and emits bright green fluorescence.[17] In the proof-of-concept of the proposed EV-based functional assay, the accumulation of fluorescein inside EVs is a measure of two independent parameters: enzymatic activity and membrane integrity. So, in a first pilot test, we incubated a fixed amount of nanoalgosomes (10^{11} EVs/ml) with FDA (35 µmol). Next, we checked if there was a detectable fluorescence intensity emission with respect to a negative control which correspond to nanoalgosome vehicle solution (i.e., phosphate saline buffer solution, PBS), using spectrofluorometer readings. The fluorescence emission was followed over time, up to 16 hours (960 min, **Figure 3**). Interestingly, we got a rapid determination of active EV-related enzymes, resulting in a time-dependent increase of fluorescence intensity only in the nanoalgosome samples. Based on this preliminary result, fundamental parameters like the temperature (around 22°C, room temperature) and the duration of the assay were defined, setting it equal to 3 hours (time during which the reaction is within the exponential phase, away from the plateau), in order to make the test rapid and sufficiently sensitive.

Set-up of functional enzymatic assays for extracellular vesicles

For the validation of analytical procedures, it is important to establish key parameters such as specificity, accuracy, and precision.[35] Initially, we gated the appropriate approach to develop a functional assay for EVs that provides a universally quantifiable and standardizable final value. To accomplish that and to accurately determine the amount of FDA that is enzymatically cleaved during the assay, standards play a crucial role. The original FDA-related method for preparing standards involved boiling different concentration of FDA solutions in a water bath. However, according to J. Schnürer et al, 1982 and G. Adam et al, 2001, this method consistently underestimated the amount of FDA hydrolyzed during standard preparation.[36,16] Therefore, a commercially available sodium fluorescein salt was chosen to prepare reliable standard calibration curve.

This method allows for a direct measurement of enzymatic activity by deriving the amount of fluorescein released per minute during the functional assay. Moreover, standards prepared using this method remained consistent over three months.[16] Figure 4a shows the fluorescein calibration curve obtained through serial dilutions of a stock solution of fluorescein, measured by relative fluorescence intensity emission at 516 nm. The calibration curve obtained shows a linear trend (**figure 4a**), which enables the easy conversion of fluorescence intensity emission (after FDA hydrolysis) into nmol of fluorescein produced, after the enzymatic reaction. In addition, to establish a robust enzymatic-based assay, we employed the Michaelis-

Menten model, one of the most widely used approaches for studying enzyme kinetics.[37,38,39]

We applied this method to determine the kinetic parameters of enzymes present in EV-cargo, performing the enzymatic study at increasing substrate concentrations to measure the initial reaction rate at constant EV concentrations ($5x10^{10}$/ml). As shown in **figure 4b**, by plotting reaction rates against substrate concentration, we obtained a canonical hyperbolic relationship. Applying a nonlinear regression to the Michaelis-Menten equation, we obtained the kinetic parameters, including the maximum reaction velocity (Vmax) and the kinetic constant (Km) in the Michaelis-Menten model (**Figure 4b**).

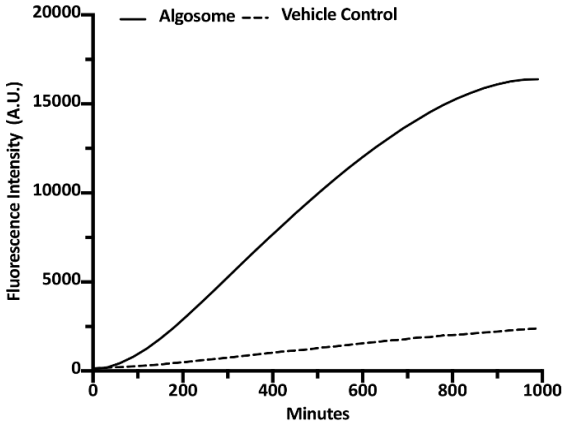

Figure 3. Graph of time-dependent increase of fluorescence emission intensity (expressed in arbitrary units) in microalgal-derived extracellular vesicles (nanoalgosomes) incubated with FDA, compared to a negative control (vehicle control).

The steady-state kinetics provides a simple and rapid means of assessing the specificity of the substrate-enzyme complex.[40] The specific enzyme kinetic constants were calculated as the best fit values, with a Vmax equal to 2.9 nmol/min and a Km equal to 3 µmol, validating the high-affinity enzymes found in nanoalgosomes for the FDA substrate. These values suggest the substrate concentration should be chosen to ensure that the enzyme is acting near Vmax.[37] Typically, a substrate concentration higher than the Km value is used for enzymatic activity studies.[37] Based on these evidences, we decided to fix the FDA substrate concentration 6-fold higher than Km, at 18 µmol.[39,41] Further, the specific enzymatic activity is internationally expressed as enzymatic unit (U), in which 1 U is the quantity of enzyme required to catalyze the conversion of one nanomole of substrate into product per minute (nmol/min), under the assay method's stated conditions.[42] We have adopted the enzymatic unit to quantitatively define the EV-related enzymatic activity. This is done by calculating the amount of fluorescein produced per minute through interpolation with the standard curve.

In order to establish the analytical sensitivity, we determined the detection limit of the functional assay by identifying the lowest concentration of EVs to be used that could be distinguished from the background noise (v/v of PBS solution incubated with FDA). Therefore, to determine the detection limit, we incubated different nanoalgosome concentrations of the same preparation batch (ranging from $1x10^{11}$ to $6x10^{8}$ EVs/ml) with FDA. We found that the enzymatic assay is dose-responsive, with a detection limit of $6.25x10^{9}$ EVs/ml or above (**Figure 5a**).

Moreover, to verify if the analytical specificity of the functional assay is related to the bioactivity of active enzymes inside intact EVs, we used a nonionic detergent, Triton X100, which permeabilizes lipid membrane bilayers but does not affect protein bioactivity, like enzymatic activity. As established in our previous study, we induced nanoalgosome lysis by treatment with 1% Triton-X 100 for 30 minutes.[1] The results of the functional assay showed in **figure 5b** indicated that the measurable fluorescent signal is dependent on active enzymes of intact EV samples. Indeed, we detected enzymatic activity only in the non-permeabilized nanoalgosomes compared to the permeabilized ones where no fluorescence signal was detected. This indicates that the functional assay is a suitable method for exclusively detecting the bioactivity of intact EVs. The same results were obtained when EVs were lysed after boiling at 100°C for 10 min, confirming the specificity of the functional assay proposed here (figure

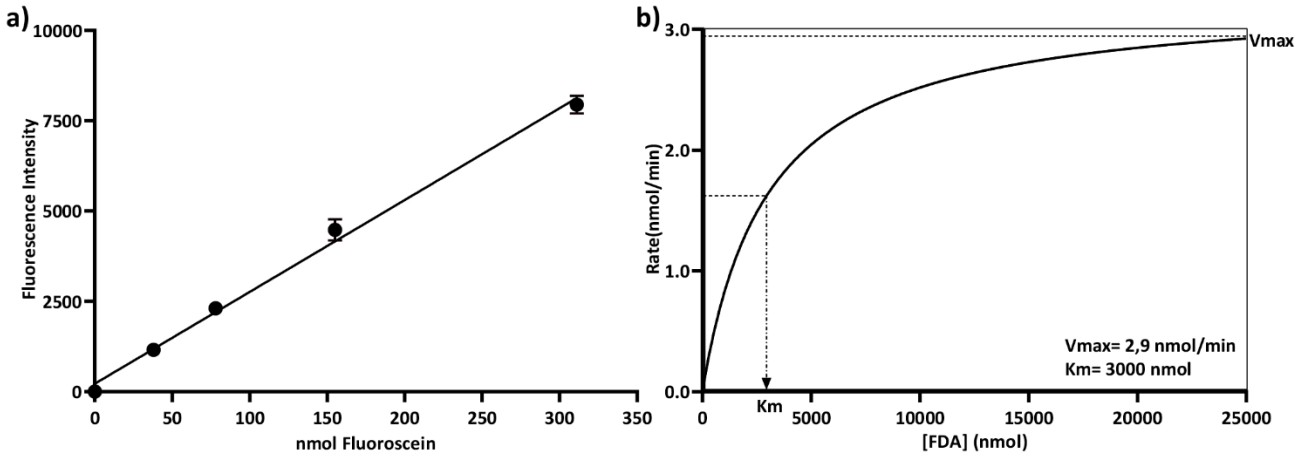

Figure 4. a) Linear calibration curve of fluorescein. b) Michaelis-Menten graph for the enzymatic cleavage of FDA catalysed by algosome enzymes.

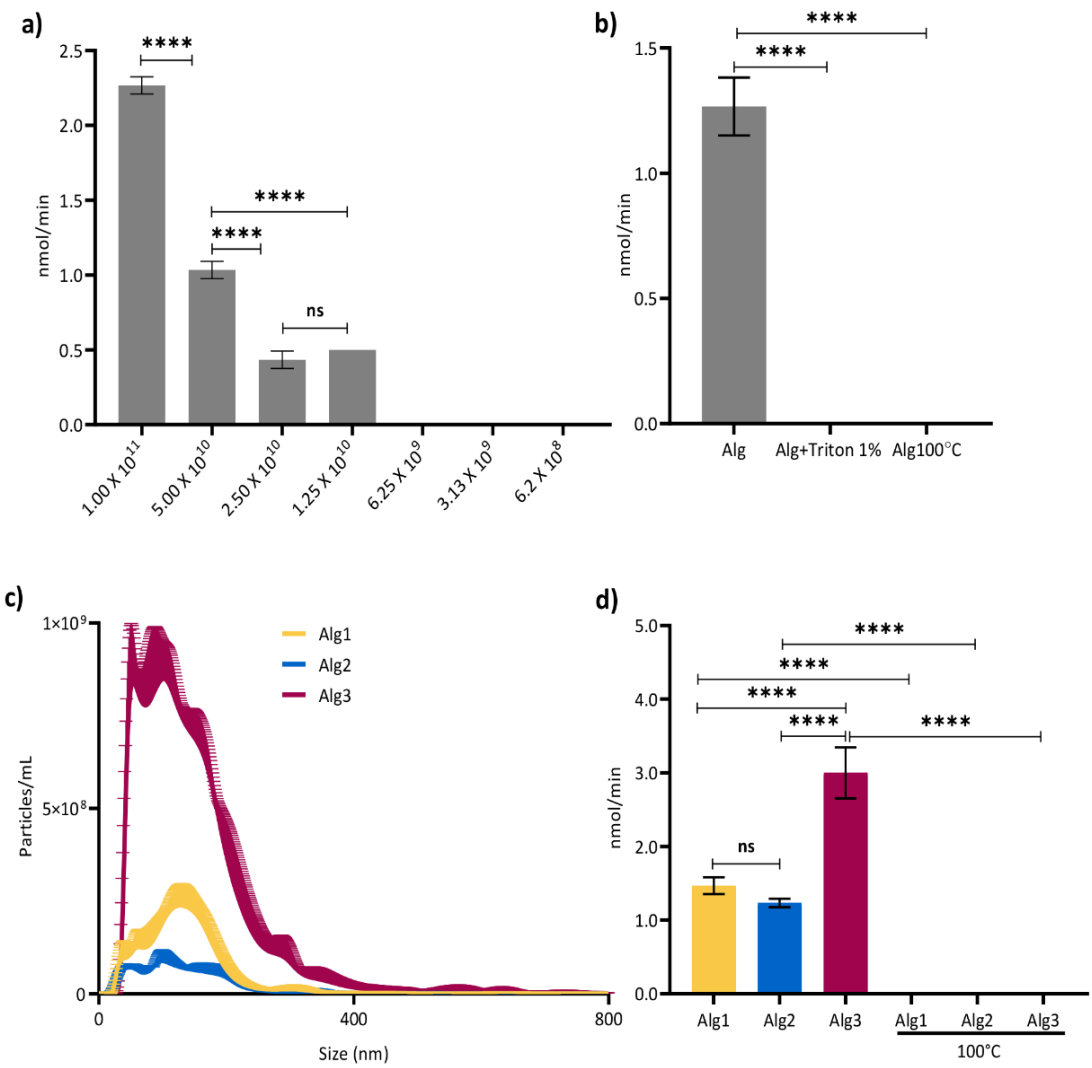

Figure 5. Set up of functional enzymatic assay on nanoalgosomes using a) different concentrations of nanoalgosomes (from $1x10^{11}$ to $6x10^{8}$ sEVs) for detection limit determination; One-way ANOVA was used to assess the statistical significance of the differences: ****p < 0.0001, ns=not significant b) nanoalgosomes, treated or untreated with detergent (1% TritonX100), or boiled at 100°C; ; One-way ANOVA was used to assess the statistical significance of the differences: Alg *vs* Alg+Triton1% and Alg *vs* Alg+100°C, ****p < 0.0001 c) F-NTA analysis; d) functional assay on nanoalgosomes from different batches (Alg1, Alg2, Alg3). One-way ANOVA was used to assess the statistical significance of the differences: ****p < 0.0001, ns=not significant.

5b). Next, we applied the proposed functional enzymatic assay, focusing on qualitative assessment of EV preparation, as to ensure batch-to-batch reliability/reproducibility for subsequent applications. As reported previously (in Adamo G. et al 2021 and in Paterna A. et al 2021), we optimized the renewable/large-scale nanoalgosome production using tangential flow filtration methods and by evaluating suggested MISEV2018 quality parameters.[1,10,43] These include extensive biophysical and biochemical characterization by different techniques, such as dynamic light scattering (DLS), nanoparticle tracking analysis in scattering and fluorescence (NTA and F-NTA), bicinchoninic acid assay (BCA assay), immunoblot (IB) analysis of EV-protein biomarkers and atomic force microscopy (AFM).[1,43] The application of EV-based quality control methods for each nanoalgosome production has allowed for the monitoring of differences in term of quality between nanoalgosome batches. These differences were mainly attributed to the performance of the TFF cartridges, which depend on their half-life.[44] In this context, we selected three nanoalgosome batches (named Alg1, Alg2, Alg3) that showed differences during the quality-control analyses (Supporting Information, S1).[43,45] To reach this aim, we performed F-NTA after staining nanoalgosomes with Di-8-ANEPPS, a specific lipophilic fluorescent dye that helps to discriminate between EVs and non-vesicle co-isolates.[1] As reported in **figure 5c**, the F-NTA results showed that the selected three batches had difference in terms of Di-8-ANEPPS-positive EVs. Interestingly, we applied the functional enzymatic assay to test its ability to highlight batch-to-batch variation between EV-preparations. The results shown in Figure 5d identified the Alg3 batch as the one with high enzymatic activity compared to the other two batches analyzed. These

findings were consistent with the F-NTA results and the quality control analyses (**Figure 5c**, **Supporting Information, S1**). These results support the proposed functional enzymatic assay as a new single-step method for validating EV preparations and monitoring batch-to-batch variability during EV production. Notably, this assay does not require washing steps, making it a faster and cost-effective method that offers several advantages, including simplicity and sensitivity.

Application of functional enzymatic assay for a wide range of experimental conditions

different storage conditions on nanoalgosomes, including 4°C, -20°C, -80°C, lyophilization in 5% and 8% sucrose (**figure 6a)**. After one week of storage, we also performed NTA to monitor the size distribution and concentration of nanoalgosomes stored under these different conditions (**figure 6b**). We observed no changes in size distribution with an average size of 100±20 nm and a quite similar nanoparticle concentrations between the samples. Conversely, as reported in **figure 6a**, the proposed functional assay highlighted a significant and quantifiable reduction in EV-bioactivity, reflecting lower enzymatic activity in frozen (-20°C or -80°C) or lyophilized EV-samples, compared to those stored at 4°C for after a week.

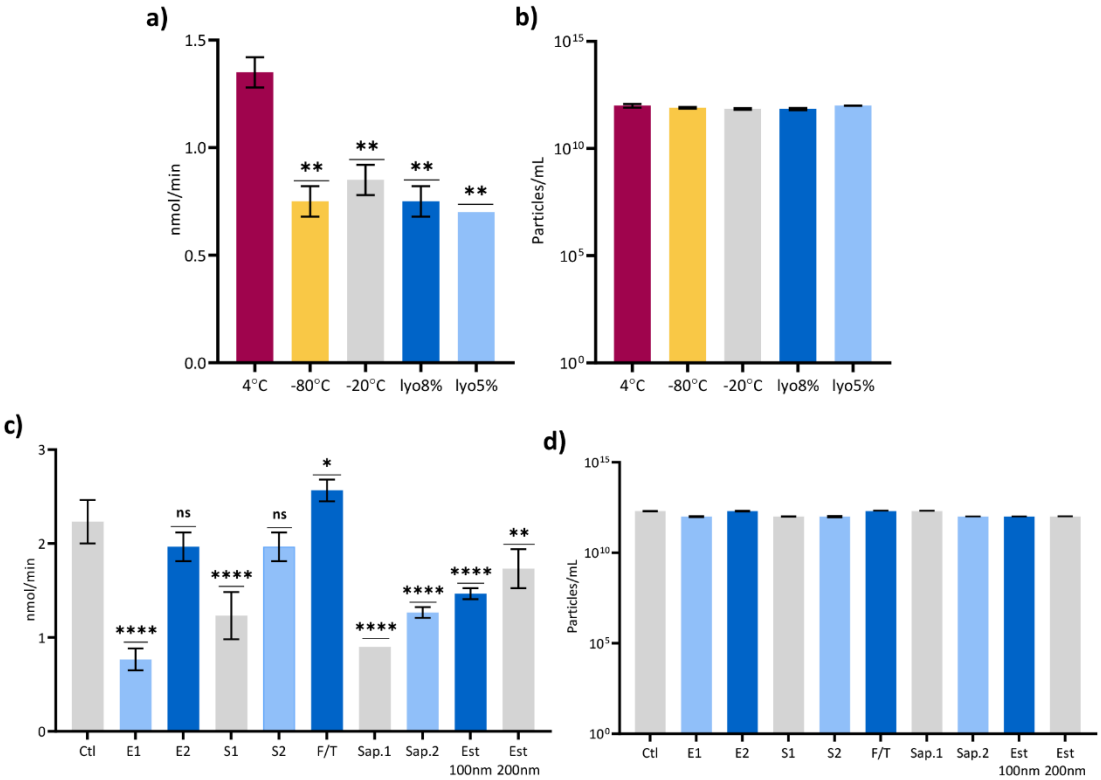

Figure 6. a-b) Effect of different storage conditions on nanoalgosomes analyzed by functional assay (nmol/min) and NTA (particles/ml); One-way ANOVA was used to assess the statistical significance of the differences 4°C vs (-80°C, -20°C, lyo8%, lyo5%, **p < 0.01. c-d) Effect of different loading methods on nanoalgosomes analyzed by functional assay (nmol/min) and NTA (particles/ml); One-way ANOVA was used to assess the statistical significance of the differences: Ctl vs (E1, S1, Sap.1, Sap.2 Est100nm), ****p < 0.0001; Ctl vs (E2, S2), ns=not significant; Ctl vs F/T, *p < 0.05; Ctl vs Est200nm, **p < 0.01

Storage conditions: The effects of different storage conditions on EVs have been investigated in several studies, demonstrating how various factors related to storage can affect EV characteristics, including membrane stability and EV potency.[46] Recently, more comprehensive studies have systematically compared different storage strategies over time to identify appropriate conditions for stabilizing EV preparations, especially for therapeutic applications.[47] Following the storage of EV samples, they are usually analysed over time using various methods, including NTA, bead-based multiplex flow cytometry, and single vesicle imaging flow cytometry (IFCM).[47] Here, we applied the functional assay to compare the effects of

These results demonstrate that the functional assay presented here can efficiently identify a decrease in the biological functionality of enzymes within EV preparations. As a result, it can predict whether an EV preparation could be suitable for future application in specific potency tests.[11,12]

Loading methods: Several studies have reported advantages of using EVs as drug delivery systems in preclinical models because of their low toxicity, high targeting capacity, and slow clearance.[48] Exogenous cargo can be loaded into EVs using various physical methods, including electroporation, sonication, saponin-assisted

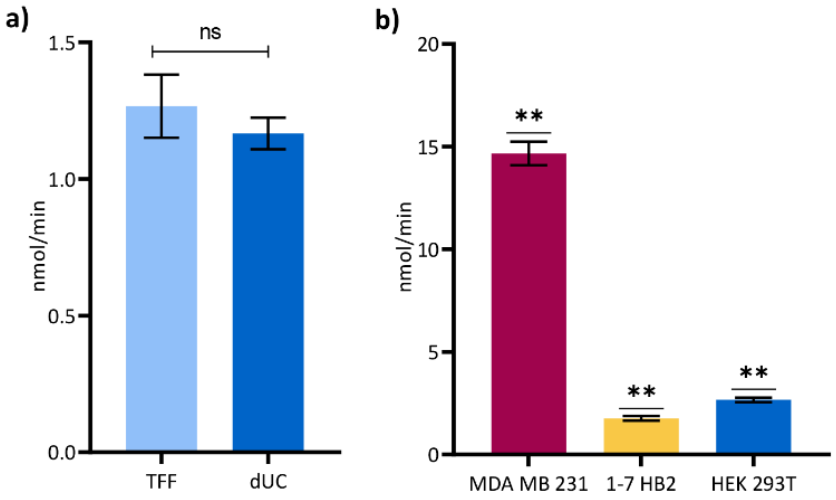

Figure 7. a) Application of functional assay on nanoalgosomes after different isolation methods and b) on sEVs from human cell lines (MDA MB 231, 1-7 HB2, HEK 293T). One-way ANOVA was used to assess the statistical significance of the differences: TFF vs dUC, ns=not significant; MDA MB 231 vs 1-7 HB2, ***p < 0.001; MDA MB 231 vs HEK 293T, ***p < 0.001; 1-7 HB2 vs HEK 293T, *p<0.05.

loading, freeze-thaw cycles, and extrusion.[49,50,51,52,53,54] However, these methods may cause a loss of EV-functionality or damage the integrity of the EV-membrane, even though the phospholipidic bilayer should quickly recover its reclosed integrity after membrane perturbations. In this context, we investigated whether the proposed functional assay could be applied to this type of assessment, testing if it could provide indications of changes or alterations in the biological properties of EVs post-loading (**figure 6c**).[55,56] To this end, different loading methods were applied to identify the optimal one(s) with minimal impact on the integrity and bioactivity of EVs.[57,58] For each method, we used the most commonly reported EV loading setting.[59,5] Contextually, we monitored changing in nanoalgosomes size distribution and concentration after the application of loading method, using NTA (**figure 6d**). In **Figure 6c**, we report the functional assay results, which highlight that freeze and thaw approach appear to be the "gentlest" loading method, with less impact on nanoalgosome features according to NTA measurements. However, for some conditions used such as electroporation (E1), sonication (S1), saponification (Sap1-2), or extrusion, we observed a significant decrease in EV-enzymatic activity, probably due to strong membrane perturbation or loss of vesicle integrity. Interestingly, this difference could not be detected by NTA analysis, as the size (inside the range of 80-100+/-20 nm for all samples) and concentration of these samples were similar with the control (**Figure 6d**). The successful application of the functional assay for evaluating EVs during loading could be the starting point for developing effective EV-based therapeutics, which might require further investigation in tailoring specific potency assays.

Comparison between EV-isolation methods: EVs derived from different bioresources can be isolated using various approaches. Depending on individual experimental settings (such as small or large-scale production), it is essential to establish the most efficient method for sEV separation while also considering the quality of the EV sample obtained. In Adamo et al. 2021, we demonstrated that different separation procedures (e.g., dUC, TFF, and gUC) allowed us to isolate nanoalgosomes from *Tetraselmis chuii* (*T. chuii*) conditioned media. In this study, we applied the functional assay to compare the quality of nanoalgosomes obtained from the same *T. chuii* culture batch, isolated in parallel by dUC and TFF.[1,60] The results indicated that nanoalgosomes isolated by either method showed the same enzymatic activity and membrane integrity, confirming the good quality of both nanoalgosome preparations (**Figure 7a**).
We can conclude that by using the proposed functional enzymatic assay, we were able to directly and quantitatively compare EV quality across the two isolation methods, different storage and loading conditions.

Functional enzymatic assay in human sEVs

Despite the well-documented techniques for characterizing EVs in human biofluids for diagnostic and therapeutic purposes, there is still a need for improved characterization methods.[61] These methods should be versatile, robust, and sensitive enough to detect smaller amounts of EVs. To test if the FDA-based functional assay fits these criteria, we verified its sensitivity, compatibility, and specificity for different EV types, including human EVs. Since EV composition depends on the producer cell type, it is reasonable to assume that the FDA-based functional assay can be applied for characterizing different types of vesicles. Therefore, we used dUC to isolate sEVs from different human cell lines, specifically normal and tumoral mammary epithelial cells, and human embryonic kidney

cells. After biochemical and biophysical characterization of these three types of sEVs, we incubated the established amount with FDA to perform the functional assay. The results in **figure 7b** confirmed the presence of reliable enzymatic-dependent activity for all three EV types analyzed, demonstrating the functional assay's compatibility with human EVs. Interestingly, breast tumor-derived sEVs showed significantly higher enzymatic activity (five-fold increase) compared to sEVs isolated from normal breast cells, opening new perspectives for the functional assay's application in tumor diagnosis.
In summary, we have developed and validated a new method that can be widely useful in the EV field, with countless applications that allow for specific EV functional evaluation from different species and possible pathological conditions.

Experimental

Microalgae cultivation

A stock culture of the microalgae *T. chuii* (CCAP 66/21b), grown in borosilicate glass bottles in modified f/2 medium (Guillard, 1975), was used to start new cultures in bottles via a 25% v/v inoculum. Cultures were kept for 4 weeks at a temperature of 22°C ± 2°C under continuous air flow and exposed to white light with a photoperiod of 14 h light and 10 h dark. Bottles were gently shaken every 2 days in order to homogenize the cultures. Microalgae were cultured in sterile conditions by using 0.22 µm filters at the bottle inlets. Cell growth was monitored every week by optical density at 600 nm and cell counting.

Mammalian cell cultivation

The following cell lines were used for EV production: (i) 1–7 HB2, normal mammary epithelial cells; (ii) MDA-MB 231, human breast cancer epithelial cells; and (iii) HEK 293T, human embryonic kidney cells. MDA-MB-231 and HEK293T were cultured in Dulbecco's Modified Eagle Medium (DMEM, Sigma-Aldrich) containing 10% (v/v) Fetal Bovine Serum (FBS, Gibco, Life Technologies) plus 2 mM L-glutamine, 100 U/ml Penicillin and 100 mg/ml Streptomycin (Sigma-Aldrich); instead, the 1–7 HB2 cell line was cultured in low-glucose DMEM (Sigma-Aldrich) containing 10% (v/v) Fetal Bovine Serum, plus 2 mM L-glutamine, 100 U/ml Penicillin and 100 mg/ml Streptomycin, 5 µg/ml Hydrocortisone (Sigma-Aldrich) and 10 µg/ml Bovine Insulin (Sigma-Aldrich). All cell lines were maintained at 37°C in a humidified atmosphere (5% CO_2). All cell lines were seeded in 175 cm² flasks until 70% confluence was reached. Next, cells were washed twice with phosphate saline buffer (PBS, Sigma- Aldrich) with Ca^{++} and Mg^{++} and cultured in appropriate medium supplemented with 10% of EV-depleted FBS. After 48 h, sEVs were isolated from each cell-conditioned medium.

Microalgae and human-derived-EV isolation

Differential ultracentrifugation. The isolation of both human cell and microalgal derived-EVs was performed by dUC, as described in Picciotto et al., 2021.[60] Briefly, conditioned media was subjected to serial centrifugation steps at 4 °C. The first was at 300 x g for 10 min. The collected supernatant was subjected to 2,000 x g for 10 min to remove all cell debris. Large EVs (lEVs) were separated in 50 ml Eppendorf polypropylene conical tubes at 10,000 × g for 30 min at 4°C using an Eppendorf rotor F34-6-38. We then collected sEVs from the supernatant into Beckman Coulter polypropylene open top tubes via centrifugation at 118,000 × g for 70 min at 4°C using a Beckman SW28 rotor. After a PBS washing step, the pellet was re-suspended in PBS without Ca^{++} and Mg^{++} for subsequent analyses.
Tangential flow filtration. Isolation of microalgal derived-EVs was performed using the KrosFlo® KR2i TFF System from Repligen (Spectrum Labs., Los Angeles, CA, USA) and three modified polyethersulfone hollow fiber membranes (S04-E65U-07-N, S04-P20-10-N and S04-E500-10-N, Spectrum Labs). Briefly, microalgae cultures were purified by microfiltration and ultra-filtration using a hollow fiber cartridge housed in the KrosFlo® KR2i, with cut-offs of 650 nm (S04-E65U-07-N, Spectrum Labs), 200 nm (S04-P20-10-N, Spectrum Labs), and 500-kDa (S04-E500-10-N, Spectrum Labs). Feed flow and transmembrane pressure (TMP) were kept constant at 450 ml/min and 0.05 bar, respectively.
The small and large EVs recovered from the retentate of the 500 kDa and 200 nm cut-off TFF filter modules, respectively, were concentrated until a final volume of approximately 150 ml. Subsequently, using a smaller 500 kDa cut-off TFF filter module (C02-E500-10-N, Spectrum Labs, MicroKros) with a feed flow of 75 ml/min and a permeate flow of 2 ml/min, samples were further concentrated and diafiltrated seven times with PBS, without Ca^{++} and Mg^{++}, reaching a final volume of approximately 5 ml.

EV characterization

Nanoparticle tracking analysis. Particle concentration and size distributions of EVs were measured using an NTA instrument (NanoSight NS300, Malvern Panalytical, UK).
EV samples were diluted to generate a dilution in which 20–120 particles per frame were tracked, to obtain a concentration within the recommended measurement range (1 - 10 × 10^8 particles/ml). For each individual sample, five videos of 60 s were recorded and analyzed with detection threshold 5 and camera level 15-16. All videos were analyzed by NTA Software.

Fluorescent-nanoparticle tracking analysis. EVs were stained with 500 nm of 4-(2-[6-(diethylamino)-2-naphthalenyl]ethynyl)-1-(3 sulfopropyl) pyridinium, DI-8-ANEPPS (Ex/Em: 467/631 nm, Thermo Fisher Scientific), previously filtered by 20 nm filters (Whatman Anotop filters), whose fluorescence is activated in a-polar enviro nments, and specifically enhanced when bound to the lipid membrane of EVs, with a higher quantum yield concerning any binding to hydrophobic protein regions.
This makes the Di-8-ANEPPS fluorescent signal highly EV-specific. After 1 h at room temperature, F-NTA analyses were carried out as described in Adamo et al., 2021.[1]
Protein quantification. Total protein was quantified using the microBCA protein assay kit (Thermo Fisher Scientific) according to the manufacturer's instructions, using bovine serum albumin (BSA) as a standard.
Then, the EV samples and standards were mixed with the working reagent and incubated for 1 h at 37°C. Absorbance values were measured at 562 nm, using a GloMax® Discover Microplate Reader.

Set up of functional enzymatic assay: pilot test

Fluorescein diacetate (FDA, Sigma-Aldrich) stock solution was prepared in acetone at a final concentration of 2 mg/. 10^{11}/ml nanoalgosomes were incubated with 35 µmol of FDA, reaching a final volume of 200 µl with 0.2 µm filtered PBS without Ca^{++} and Mg^{++}.
The same amount of FDA was added to 0.2 µm filtered PBS without Ca^{++} and Mg^{++} (nanoalgosome-vehicle). Fluorescence emission was followed up to 16 h, using a blue filter of the GloMax Discover Microplate Reader.
Preparation fluorescein standards curve. Fluorescein sodium salt (ex/em 490/514 nm, Sigma-Aldrich) was used to generate a standard calibration curve.
The fluorescence intensity of serial dilutions of fluorescein (from 300 nmol to 0 nmol), diluted in PBS without Ca^{++} and Mg^{++} at a final volume of 200 µl, was measured in a 96-well-plate using a blue filter of the GloMax Discover Microplate Reader (Promega).

Michaelis–Menten Kinetic

5 × 10^{10}/ml nanoalgosomes were incubated with different concentrations of FDA (0, 1.6, 3.3, 6.6, 13, 26 x 10^3 nmol) dissolved in 0.2 µm filtered PBS without Ca^{++} and Mg^{++}, in a final volume equal to 200 µl. The fluorescence emission was followed until 3 hours, in a 96-well-plate using a blue filter of the GloMax Discover Microplate Reader (Promega). Obtained values were corrected by subtracting background fluorescence value (i.e., PBS with FDA). Fitting these data to the standard calibration curve, the Michaelis–Menten equation was applied using nonlinear regression and plotting the reaction's initial rates (µmol/min) as a function of FDA concentration. Vmax and Km were found using GraphPad software.

Functional enzymatic assay for EVs

Measure of enzymatic activity. To calculate the specific enzymatic activity, the enzyme unit (U), the amount of enzyme that catalyses the reaction of 1 nmol of substrate into product per minute, was determined. Thus, for the functional assay, EV-enzymatic activity values were expressed in units as nmol of fluorescein produced per minute (nmol/min). This value was obtained by fitting the fluorescence intensities measured during the functional assay with the fluorescein concentration of the standard curve.
Analytical sensitivity. Serial dilutions of nanoalgosomes (from 5 × 10^{10}/ml to 6.2 × 10^8/ml sEVs) were incubated with 18 µmol of FDA, reaching a final volume of 200 µl with 0.2 µm filtered PBS without Ca^{++} and Mg^{++}. Fluorescence emission was followed up to 3h, using a blue filter of the GloMax Discover Microplate Reader. The same amount of FDA was added to 0.2 µm-filtered PBS without Ca^{++} and Mg^{++} (nanoalgosome-vehicle). This background fluorescence value was subtracted from the fluorescence intensity values of each sample, for all the condition described.
Analytical specificity. 5 × 10^{10}/ml nanoalgosomes were incubated with 1% Triton X-100 (Sigma-Aldrich) for 30 min at room temperature. The same amount of nanoalgosomes were boiled at 100°C for 10 min. Next, samples were incubated with 18 µmol of FDA, reaching a final volume of 200 µl with 0.2 µm filtered PBS without Ca^{++} and Mg^{++}. Fluorescence emission was followed up to 3h, and enzymatic activity was determined as described previously. As control, the same amount of FDA was added to 0.2 µm-filtered PBS without Ca^{++} and Mg^{++} boiled at 100°C for 10 min or with 1% Triton X-100. This background fluorescence value was subtracted from the fluorescence intensity values of each respective sample.
Batch-to-batch reproducibility. 5 × 10^{10}/ml nanoalgosomes from different batches (named Alg1, Alg2, and Alg3) were incubated with 18 µmol of FDA, reaching a final volume of 200 µl with 0.2 µm filtered PBS without Ca^{++} and Mg^{++}. Fluorescence emission was followed up to 3h, and enzymatic activity was determined as described above. As negative controls, nanoalgosomes were boiled at 100°C for 10 min.

Application of functional assay

Storage conditions. Nanoalgosomes were stored for 10 days at different condition: 4°C, -20°C, −80 °C and upon lyophilization in 5% and 8% sucrose for a week. Lyophilized samples were carefully rehydrated in 0.2 µm-filtered Milli-Q water and vortexed to ensure complete re-dispersion. After NTA analysis on all stored samples, an

enzymatic functional assay was performed, as described previously.

Loading methods. 2 x 10^{12}/ml nanoalgosomes (and nanoalgosome-vehicle, *i.e*. 0.2 µm filtered PBS without Ca^{++} and Mg^{++}, used as a negative control) underwent the subsequent treatments:

-Electroporation was performed in Gene Pulser cuvettes (0.4 cm cell electrode gap) on a BioRad Gene Pulser equipped with a capacitance extender, with two conditions selected, E1 (125 µF, 400 V and 2 pulse time of 20 ms) and E2 (125 µF, 250 V and 2 pulse time of 30 ms).

Sonication was performed using two settings: sonicator (S1) with 20% amplitude for six cycles of 30 seconds on/off for a total of 3 min, with 2 min cooling, then incubation for 60 min at 37°C; ultrasonic bath (S2) 40 KHz, 40% amplitude for 2 cycles of 30 seconds on/off, then incubation for 60 min at 37°C.

-Freeze–Thaw was performed in 3 cycles of freezing at -80° for 30 min and thawing at room temperature (RT) for 30 min.

-Saponification was performed using two settings: incubation with 0.1 mg/ml (Sap1) and 0.002 mg/ml (Sap2) of saponin (Sigma-Aldrich) at RT for 10 min.

-Extrusion using a syringe-based hand-held mini-extruder equipped with polycarbonate membranes of 100 nm and 200 nm pore size (Track-Etched Membrane, Whatman). Each sample was extruded 31 times.

After the application of each method, NTA analysis was performed on all samples. Next, the enzymatic functional assay was performed, as described previously.

Isolation methods. 5 × 10^{10}/ml nanoalgosomes of the same batch, isolated by dUC and TFF, were used to perform the functional enzymatic assay, as described before.

Functional assay in human-derived sEVs

5 × 10^{10}/ml sEVs isolated from MDA MB231, 1-7 HB2, and HEK 293T cells were employed to conduct the functional enzymatic assay, using the same experimental setting described for nanoalgosomes.

Statistical analysis

Each measurement reported here was repeated as experimental triplicate, and mean values, as well as standard deviations, were calculated.

One-way ANOVA analysis was performed using GraphPad software.

Conclusions

Even though MISEV2018 set the rules for the harmonization of EV nomenclature and characterization, the need for standardization of functional or potency assays has become an important issue. Specifically, functional assays that may be or be developed into potency assays are needed to fill this gap.[10,62,63,64,65] Many *in vivo* and *in vitro* assays are currently in use to assess the effective potency of EVs to elicit a specific therapeutic effect. Although such assays are crucial for understanding EV-bioactivity, they are not formally applicable as universal functional assays. Ideally, a functional result should be expressed as a 'Functional Unit', which is a dose of EVs at which a specific, quantifiable (biological) activity is elicited.[66] Here, we propose a new functional enzymatic assay that allows the simultaneous evaluation of the bioactivity and integrity of EVs in a single step analysis. Our functional assay is simple, fast, and cost-effective, resulting in a reliable and quantifiable value expressed as enzymatic unit, starting from a small-size of EV-samples. Moreover, this study lays the foundations for the extension into other similar enzymatic functional tests for EVs based on the methods described here, but using FDA-like molecules already used for flow cytometry analysis or other specific substrate for enzymes present in EV-cargo. Beyond the evaluation of EV-integrity and bioactivity, our functional test demonstrated high potential to cover countless applications in EV-field. An example could be its application as a new, sensitive diagnostic test for routine screening analysis to assess the presence of tumoral-EVs from different sources, like plasma or urine, given its high sensitivity, cost effectiveness, and the high levels of enzymatic activity reported for tumor EVs, by simply establishing a reasonable threshold value using 10^{10} vesicles. In fact, our preliminary data on EVs isolated from human normal and tumor cells encourage the extension of our functional assay in diagnostics, also given the significant difference in terms of enzymatic activity between normal and tumor EVs. In conclusion, we suggest our EV-functional assay to be adopted among the minimal analytical assays for QC assessment of EVs.

Author Contributions (CRediT)

Giorgia Adamo: Conceptualization, Methodology, Formal analysis, Visualization, Investigation, Validation, Writing - Original Draft and Review & Editing; Sabrina Picciotto: Methodology, Formal analysis, Data curation, Software, Visualization, Validation, Writing - Original Draft; Paola Gargano and Angela Paterna: Formal analysis, Data curation; Antonella Bongiovanni: Conceptualization, Investigation, Validation, Writing - Original Draft and Review & Editing, Supervision, Visualization, Project administration, Funding acquisition: Review & Editing.

Conflicts of interest

There are no conflicts to declare.

Acknowledgements

We would like to express our sincere gratitude to Professor Giulio Ghersi for his valuable biochemical suggestions.

Associated Content

Supporting information (PDF) contains additional figures, tables and detailed supplementary methods, this file is available free of charge.

Funding Sources

This work was supported by the VES4US and the BOW projects funded by the European Union's Horizon 2020 research and innovation programme, under grant agreements nos. 801338 and 952183.

Notes and references

1 G. Adamo, D. Fierli, D. P. Romancino, S. Picciotto, M. E. Barone, A. Aranyos, D. Božič, S. Morsbach, S. Raccosta, C. Stanly, C. Paganini, M. Gai, A. Cusimano, V. Martorana, R. Noto, R. Carrotta, F. Librizzi, L. Randazzo, R. Parkes, U. Capasso Palmiero, E. Rao, A. Paterna, P. Santonicola, A. Iglič, L. Corcuera, A. Kisslinger, E. D. Schiavi, G. L. Liguori, K. Landfester, V. Kralj-Iglič, P. Arosio, G. Pocsfalvi, N. Touzet, M. Manno and A. Bongiovanni, Journal of Extracellular Vesicles, 2021, 10, e12081.

2 S. Picciotto, P. Santonicola, A. Paterna, E. Rao, S. Raccosta, D. P. Romancino, R. Noto, N. Touzet, M. Manno, E. Di Schiavi, A. Bongiovanni and G. Adamo, Front Bioeng Biotechnol, 2022, 10, 830189.

3 Y. Chen, Y. Zhao, Y. Yin, X. Jia and L. Mao, Bioengineered, 2021, 12, 8186–8201.

4 T. O'Grady, M.-S. Njock, M. Lion, J. Bruyr, E. Mariavelle, B. Galvan, A. Boeckx, I. Struman and F. Dequiedt, BMC Biology, 2022, 20, 72.

5 I. K. Herrmann, M. J. A. Wood and G. Fuhrmann, Nat Nanotechnol, 2021, 16, 748–759.

6 Y. Sun, G. Liu, K. Zhang, Q. Cao, T. Liu and J. Li, Stem Cell Res Ther, 2021, 12, 561.

7 V. V. T. Nguyen, K. W. Witwer, M. C. Verhaar, D. Strunk and B. W. M. van Balkom, J Extracell Vesicles, 2020, 10, e12033.

8 A. Yekula, K. Muralidharan, K. M. Kang, L. Wang, L. Balaj and B. S. Carter, Methods, 2020, 177, 58–66.

9 S. Bruno, M. Tapparo, F. Collino, G. Chiabotto, M. C. Deregibus, R. Soares Lindoso, F. Neri, S. Kholia, S. Giunti, S. Wen, P. Quesenberry and G. Camussi, Tissue Eng Part A, 2017, 23, 1262–1273.

10 C. Théry, K. W. Witwer, E. Aikawa, M. J. Alcaraz, J. D. Anderson, R. Andriantsitohaina, A. Antoniou, T. Arab, F. Archer, G. K. Atkin-Smith, D. C. Ayre, J.-M. Bach, D. Bachurski, H. Baharvand, L. Balaj, S. Baldacchino, N. N. Bauer, A. A. Baxter, M. Bebawy, C. Beckham, A. Bedina Zavec, A. Be nmoussa, A. C. Berardi, P. Bergese, E. Bielska, C. Blenkiron, S. Bobis-Wozowicz, E. Boilard, W. Boireau, A. Bongiovanni, F. E. Borràs, S. Bosch, C. M. Boulanger, X. Breakefield, A. M. Breglio, M. Á. Brennan, D. R. Brigstock, A. Brisson, M. L. Broekman, J. F. Bromberg, P. Bryl-Górecka, S. Buch, A. H. Buck, D. Burger, S. Busatto, D. Buschmann, B. Bussolati, E. I. Buzás, J. B. Byrd, G. Camussi, D. R. Carter, S. Caruso, L. W. Chamley, Y.-T. Chang, C. Chen, S. Chen, L. Cheng, A. R. Chin, A. Clayton, S. P. Clerici, A. Cocks, E. Cocucci, R. J. Coffey, A. Cordeiro-da-Silva, Y. Couch, F. A. Coumans, B. Coyle, R. Crescitelli, M. F. Criado, C. D'Souza-Schorey, S. Das, A. Datta Chaudhuri, P. de Candia, E. F. De Santana, O. De Wever, H. A. Del Portillo, T. Demaret, S. Deville, A. Devitt, B. Dhondt, D. Di Vizio, L. C. Dieterich, V. Dolo, A. P. Dominguez Rubio, M. Dominici, M. R. Dourado, T. A. Driedonks, F. V. Duarte, H. M. Duncan, R. M. Eichenberger, K. Ekström, S. El Andaloussi, C. Elie-Caille, U. Erdbrügger, J. M. Falcón-Pérez, F. Fatima, J. E. Fish, M. Flores-Bellver, A. Försönits, A. Frelet-Barrand, F. Fricke, G. Fuhrmann, S. Gabrielsson, A. Gámez-Valero, C. Gardiner, K. Gärtner, R. Gaudin, Y. S. Gho, B. Giebel, C. Gilbert, M. Gimona, I. Giusti, D. C. Goberdhan, A. Görgens, S. M. Gorski, D. W. Greening, J. C. Gross, A. Gualerzi, G. N. Gupta, D. Gustafson, A. Handberg, R. A. Haraszti, P. Harrison, H. Hegyesi, A. Hendrix, A. F. Hill, F. H. Hochberg, K. F. Hoffmann, B. Holder, H. Holthofer, B. Hosseinkhani, G. Hu, Y. Huang, V. Huber, S. Hunt, A. G.-E. Ibrahim, T. Ikezu, J. M. Inal, M. Isin, A. Ivanova, H. K. Jackson, S. Jacobsen, S. M. Jay, M. Jayachandran, G. Jenster, L. Jiang, S. M. Johnson, J. C. Jones, A. Jong, T. Jovanovic-Talisman, S. Jung, R. Kalluri, S.-I. Kano, S. Kaur, Y. Kawamura, E. T. Keller, D. Khamari, E. Khomyakova, A. Khvorova, P. Kierulf, K. P. Kim, T. Kislinger, M. Klingeborn, D. J. Klinke, M. Kornek, M. M. Kosanović, Á. F. Kovács, E.-M. Krämer-Albers, S. Krasemann, M. Krause, I. V. Kurochkin, G. D. Kusuma, S. Kuypers, S. Laitinen, S. M. Langevin, L. R. Languino, J. Lannigan, C. Lässer, L. C. Laurent, G. Lavieu, E. Lázaro-Ibáñez, S. Le Lay, M.-S. Lee, Y. X. F. Lee, D. S. Lemos, M. Lenassi, A. Leszczynska, I. T. Li, K. Liao, S. F. Libregts, E. Ligeti, R. Lim, S. K. Lim, A. Linē, K. Linnemannstöns, A. Llorente, C. A. Lombard, M. J. Lorenowicz, Á. M. Lörincz, J. Lötvall, J. Lovett, M. C. Lowry, X. Loyer, Q. Lu, B. Lukomska, T. R. Lunavat, S. L. Maas, H. Malhi, A. Marcilla, J. Mariani, J. Mariscal, E. S. Martens-Uzunova, L. Martin-Jaular, M. C. Martinez, V. R. Martins, M. Mathieu, S. Mathivanan, M. Maugeri, L. K. McGinnis, M. J. McVey, D. G. Meckes, K. L. Meehan, I. Mertens, V. R. Minciacchi, A. Möller, M. Møller Jørgensen, A. Morales-Kastresana, J. Morhayim, F. Mullier, M. Muraca, L. Musante, V. Mussack, D. C. Muth, K. H. Myburgh, T. Najrana, M. Nawaz, I. Nazarenko, P. Nejsum, C. Neri, T. Neri, R. Nieuwland, L. Nimrichter, J. P. Nolan, E. N. Nolte-'t Hoen, N. Noren Hooten, L. O'Driscoll, T. O'Grady, A. O'Loghlen, T. Ochiya, M. Olivier, A. Ortiz, L. A. Ortiz, X. Osteikoetxea, O. Østergaard, M. Ostrowski, J. Park, D. M. Pegtel, H. Peinado, F. Perut, M. W. Pfaffl, D. G. Phinney, B. C. Pieters, R. C. Pink, D. S. Pisetsky, E. Pogge von Strandmann, I. Polakovicova, I. K. Poon, B. H. Powell, I. Prada, L. Pulliam, P. Quesenberry, A. Radeghieri, R. L. Raffai, S. Raimondo, J. Rak, M. I. Ramirez, G. Raposo, M. S. Rayyan, N. Regev-Rudzki, F. L. Ricklefs, P. D. Robbins, D. D. Roberts, S. C. Rodrigues, E. Rohde, S. Rome, K. M. Rouschop, A. Rughetti, A. E. Russell, P. Saá, S. Sahoo, E. Salas-Huenuleo, C. Sánchez, J. A. Saugstad, M. J. Saul, R. M. Schiffelers, R. Schneider, T. H. Schøyen, A. Scott, E. Shahaj, S. Sharma, O. Shatnyeva, F. Shekari, G. V. Shelke, A. K. Shetty, K. Shiba, P. R.-M. Siljander, A. M. Silva, A. Skowronek, O. L. Snyder, R. P. Soares, B. W. Sódar, C. Soekmadji, J. Sotillo, P. D. Stahl, W. Stoorvogel, S. L. Stott, E. F. Strasser, S. Swift, H. Tahara, M. Tewari, K. Timms, S. Tiwari, R. Tixeira, M. Tkach, W. S. Toh, R. Tomasini, A. C. Torrecilhas, J. P. Tosar, V. Toxavidis, L. Urbanelli, P. Vader, B. W. van Balkom, S. G. van der Grein, J. Van Deun, M. J. van Herwijnen, K. Van Keuren-Jensen,

G. van Niel, M. E. van Royen, A. J. van Wijnen, M. H. Vasconcelos, I. J. Vechetti, T. D. Veit, L. J. Vella, É. Velot, F. J. Verweij, B. Vestad, J. L. Viñas, T. Visnovitz, K. V. Vukman, J. Wahlgren, D. C. Watson, M. H. Wauben, A. Weaver, J. P. Webber, V. Weber, A. M. Wehman, D. J. Weiss, J. A. Welsh, S. Wendt, A. M. Wheelock, Z. Wiener, L. Witte, J. Wolfram, A. Xagorari, P. Xander, J. Xu, X. Yan, M. Yáñez-Mó, H. Yin, Y. Yuana, V. Zappulli, J. Zarubova, V. Žėkas, J.-Y. Zhang, Z. Zhao, L. Zheng, A. R. Zheutlin, A. M. Zickler, P. Zimmermann, A. M. Zivkovic, D. Zocco and E. K. Zuba-Surma, J Extracell Vesicles, 2018, 7, 1535750.

11 K. Pachler, N. Ketterl, A. Desgeorges, Z. A. Dunai, S. Laner-Plamberger, D. Streif, D. Strunk, E. Rohde and M. Gimona, Int J Mol Sci, 2017, 18, 1413.

12 M. Gimona, M. F. Brizzi, A. B. H. Choo, M. Dominici, S. M. Davidson, J. Grillari, D. M. Hermann, A. F. Hill, D. de Kleijn, R. C. Lai, C. P. Lai, R. Lim, M. Monguió-Tortajada, M. Muraca, T. Ochiya, L. A. Ortiz, W. S. Toh, Y. W. Yi, K. W. Witwer, B. Giebel and S. K. Lim, Cytotherapy, 2021, 23, 373–380.

13 M. I. Ramirez, M. G. Amorim, C. Gadelha, I. Milic, J. A. Welsh, V. M. Freitas, M. Nawaz, N. Akbar, Y. Couch, L. Makin, F. Cooke, A. L. Vettore, P. X. Batista, R. Freezor, J. A. Pezuk, L. Rosa-Fernandes, A. C. O. Carreira, A. Devitt, L. Jacobs, I. T. Silva, G. Coakley, D. N. Nunes, D. Carter, G. Palmisano and E. Dias-Neto, Nanoscale, 2018, 10, 881–906.

14 D. Zheng, H. Ruan, W. Chen, Y. Zhang, W. Cui, H. Chen and H. Shen, Bioactive Materials, 2023, 25, 500–526.

15 E. Sırt Çıplak and K. G. Akoğlu, Heritage, 2020, 3, 671–681.

16 G. Adam and H. Duncan, Soil Biology and Biochemistry, 2001, 33, 943–951.

17 D. A. Fontvieille, A. Outaguerouine and D. R. Thevenot, Enviro nmental Technology, 1992, 13, 531–540.

18 F. Ender, P. Zamzow, N. von Bubnoff and F. Gieseler, International Journal of Molecular Sciences, 2020, 21, 291.

19 W. D. Gray, A. J. Mitchell and C. D. Searles, MethodsX, 2015, 2, 360–367.

20 V. Pospichalova, J. Svoboda, Z. Dave, A. Kotrbova, K. Kaiser, D. Klemova, L. Ilkovics, A. Hampl, I. Crha, E. Jandakova, L. Minar, V. Weinberger and V. Bryja, Journal of Extracellular Vesicles, 2015, 4, 25530.

21 L. de Rond, E. van der Pol, C. M. Hau, Z. Varga, A. Sturk, T. G. van Leeuwen, R. Nieuwland and F. A. W. Coumans, Clinical Chemistry, 2018, 64, 680–689.

22 N. Nikiforova, M. Chumachenko, I. Nazarova, L. Zabegina, M. Slyusarenko, E. Sidina and A. Malek, Membranes, , DOI:10.3390/membranes11070526.

23 T. Tertel, M. Schoppet, O. Stambouli, A. Al-Jipouri, P. F. James and B. Giebel, Cytotherapy, 2022, 24, 619–628.

24 T. G. Kormelink, G. J. A. Arkesteijn, F. A. Nauwelaers, G. van den Engh, E. N. M. Nolte-'t Hoen and M. H. M. Wauben, Cytometry Part A, 2016, 89, 135–147.

25 A. Morales-Kastresana, B. Telford, T. A. Musich, K. McKinnon, C. Clayborne, Z. Braig, A. Rosner, T. Demberg, D. C. Watson, T. S. Karpova, G. J. Freeman, R. H. DeKruyff, G. N. Pavlakis, M. Terabe, M. Robert-Guroff, J. A. Berzofsky and J. C. Jones, Sci Rep, 2017, 7, 1878.

26 M. Gonzalez-Begne, B. Lu, X. Han, F. K. Hagen, A. R. Hand, J. E. Melvin and J. R. Yates, J Proteome Res, 2009, 8, 1304–1314.

27 P. A. Gonzales, T. Pisitkun, J. D. Hoffert, D. Tchapyjnikov, R. A. Star, R. Kleta, N. S. Wang and M. A. Knepper, J Am Soc Nephrol, 2009, 20, 363–379.

28 G. Pocsfalvi, L. Turiák, A. Ambrosone, P. Del Gaudio, G. Puska, I. Fiume, T. Silvestre and K. Vékey, J Plant Physiol, 2018, 229, 111–121.

29 J. Rizzo, T. Chaze, K. Miranda, R. W. Roberson, O. Gorgette, L. Nimrichter, M. Matondo, J.-P. Latgé, A. Beauvais and M. L. Rodrigues, mSphere, 2020, 5, e00476-20.

30 D.-S. Choi, D.-K. Kim, S. J. Choi, J. Lee, J.-P. Choi, S. Rho, S.-H. Park, Y.-K. Kim, D. Hwang and Y. S. Gho, PROTEOMICS, 2011, 11, 3424–3429.

31 D. Garcia-Ceron, R. G. T. Lowe, J. A. McKenna, L. M. Brain, C. S. Dawson, B. Clark, O. Berkowitz, P. Faou, J. Whelan, M. R. Bleackley and M. A. Anderson, Journal of Fungi, 2021, 7, 977.

32 M. R. Bleackley, M. Samuel, D. Garcia-Ceron, J. A. McKenna, R. G. T. Lowe, M. Pathan, K. Zhao, C.-S. Ang, S. Mathivanan and M. A. Anderson, Frontiers in Plant Science.

33 H. M. McMillan and M. J. Kuehn, Applied and Enviro nmental Microbiology, 2022, 89, e01686-22.

34 J. Vitecek, J. Petrlova, V. Adam, L. Havel, K. J. Kramer, P. Babula and R. Kizek, Sensors, 2007, 7, 222–238.

35 Potency Tests for Cellular and Gene Therapy Products; http://www.fda.gov/BiologicsBloodVaccines/GuidanceCo mplianceRegulatoryInformation/Guida nces/default.htm.

36 J. Schnürer and T. Rosswall, Appl Environ Microbiol, 1982, 43, 1256–1261.

37 H. Bisswanger, Perspectives in Science, 2014, 1, 41–55.

38 B. Choi, G. A. Rempala and J. K. Kim, Sci Rep, 2017, 7, 17018.

39 L. Michaelis, M. L. Menten, K. A. Johnson and R. S. Goody, Biochemistry, 2011, 50, 8264–8269.

40 R. G. Duggleby and C. Wood, Biochem J, 1989, 258, 397–402.

41 R. G. Duggleby, J Theor Biol, 1979, 81, 671–684.

42 P. K. Robinson, Essays Biochem, 2015, 59, 1–41.

43 A. Paterna, E. Rao, G. Adamo, S. Raccosta, S. Picciotto, D. Romancino, R. Noto, N. Touzet, A. Bongiovanni and M. Manno, Front Bioeng Biotechnol, 2022, 10, 836747.

44 L. Paolini, M. Monguió-Tortajada, M. Costa, F. Antenucci, M. Barilani, M. Clos-Sansalvador, A. C. Andrade, T. A. P. Driedonks, S. Giancaterino, S. M. Kronstadt, R. R. Mizenko, M. Nawaz, X. Osteikoetxea, C. Pereira, S. Shrivastava, A. T. Boysen, S. I. van de Wakker, M. J. C. van Herwijnen, X. Wang, D. C. Watson, M. Gimona, M. Kaparakis-Liaskos, K. Konstantinov, S. K. Lim, N. Meisner-Kober, M. Stork, P. Nejsum, A. Radeghieri, E. Rohde, N. Touzet, M. H. M. Wauben, K. W. Witwer, A. Bongiovanni and P. Bergese, Journal of Extracellular Biology, 2022, 1, e63.

45 E. D. Sverdlov, BioEssays, 2012, 34, 873–875.

46 A. Sivanantham and Y. Jin, Life, 2022, 12, 697.

47 A. Görgens, G. Corso, D. W. Hagey, R. Jawad Wiklander, M. O. Gustafsson, U. Felldin, Y. Lee, R. B. Bostancioglu, H. Sork, X. Liang, W. Zheng, D. K. Mohammad, S. I. van de Wakker, P. Vader, A. M. Zickler, D. R. Mamand, L. Ma, M. N. Holme, M. M. Stevens, O. P. B. Wiklander and S. EL Andaloussi, Journal of Extracellular Vesicles, 2022, 11, e12238.

48 P. Gangadaran and B.-C. Ahn, Pharmaceutics, 2020, 12, 442.

49 S. Fu, Y. Wang, X. Xia and J. C. Zheng, NanoImpact, 2020, 20, 100261.

50 A. Jeyaram and S. M. Jay, AAPS J, 2017, 20, 1.

51 G. D. Kusuma, M. Barabadi, J. L. Tan, D. A. V. Morton, J. E. Frith and R. Lim, Frontiers in Pharmacology.

52 T. Lener, M. Gimona, L. Aigner, V. Börger, E. Buzas, G. Camussi, N. Chaput, D. Chatterjee, F. A. Court, H. A. Del

Portillo, L. O'Driscoll, S. Fais, J. M. Falcon-Perez, U. Felderhoff-Mueser, L. Fraile, Y. S. Gho, A. Görgens, R. C. Gupta, A. Hendrix, D. M. Hermann, A. F. Hill, F. Hochberg, P. A. Horn, D. de Kleijn, L. Kordelas, B. W. Kramer, E.-M. Krämer-Albers, S. Laner-Plamberger, S. Laitinen, T. Leonardi, M. J. Lorenowicz, S. K. Lim, J. Lötvall, C. A. Maguire, A. Marcilla, I. Nazarenko, T. Ochiya, T. Patel, S. Pedersen, G. Pocsfalvi, S. Pluchino, P. Quesenberry, I. G. Reischl, F. J. Rivera, R. Sanzenbacher, K. Schallmoser, I. Slaper-Cortenbach, D. Strunk, T. Tonn, P. Vader, B. W. M. van Balkom, M. Wauben, S. E. Andaloussi, C. Théry, E. Rohde and B. Giebel, J Extracell Vesicles, 2015, 4, 30087.

53 Á. M. Lőrincz, C. I. Timár, K. A. Marosvári, D. S. Veres, L. Otrokocsi, Á. Kittel and E. Ligeti, J Extracell Vesicles, 2014, 3, 10.3402/jev.v3.25465.

54 V. Sokolova, A.-K. Ludwig, S. Hornung, O. Rotan, P. A. Horn, M. Epple and B. Giebel, Colloids Surf B Biointerfaces, 2011, 87, 146–150.

55 Y. Han, T. W. Jones, S. Dutta, Y. Zhu, X. Wang, S. P. Narayanan, S. C. Fagan and D. Zhang, Processes, 2021, 9, 356.

56 S. Rankin-Turner, P. Vader, L. O'Driscoll, B. Giebel, L. M. Heaney and O. G. Davies, Advanced Drug Delivery Reviews, 2021, 173, 479–491.

57 M. C. Jamur and C. Oliver, Methods Mol Biol, 2010, 588, 63–66.

58 J. Van Deun, Q. Roux, S. Deville, T. Van Acker, P. Rappu, I. Miinalainen, J. Heino, F. Vanhaecke, B. G. De Geest, O. De Wever and A. Hendrix, Cells, 2020, 9, 1797.

59 C. Chen, M. Sun, J. Wang, L. Su, J. Lin and X. Yan, Journal of Extracellular Vesicles, 2021, 10, e12163.

60 S. Picciotto, M. E. Barone, D. Fierli, A. Aranyos, G. Adamo, D. Božič, D. P. Romancino, C. Stanly, R. Parkes, S. Morsbach, S. Raccosta, C. Paganini, A. Cusimano, V. Martorana, R. Noto, R. Carrotta, F. Librizzi, U. Capasso Palmiero, P. Santonicola, A. Iglič, M. Gai, L. Corcuera, A. Kisslinger, E. Di Schiavi, K. Landfester, G. L. Liguori, V. Kralj-Iglič, P. Arosio, G. Pocsfalvi, M. Manno, N. Touzet and A. Bongiovanni, Biomater. Sci., 2021, 9, 2917–2930.

61 Y. Liang, B. M. Lehrich, S. Zheng and M. Lu, Journal of Extracellular Vesicles, 2021, 10, e12090.

62 K. W. Witwer and C. Théry, J Extracell Vesicles, 2019, 8, 1648167.

63 E. Geeurickx, J. Tulkens, B. Dhondt, J. Van Deun, L. Lippens, G. Vergauwen, E. Heyrman, D. De Sutter, K. Gevaert, F. Impens, I. Miinalainen, P.-J. Van Bockstal, T. De Beer, M. H. M. Wauben, E. N. M. Nolte-'t-Hoen, K. Bloch, J. V. Swinnen, E. van der Pol, R. Nieuwland, G. Braems, N. Callewaert, P. Mestdagh, J. Vandesompele, H. Denys, S. Eyckerman, O. De Wever and A. Hendrix, Nat Commun, 2019, 10, 3288.

64 S. Roura and A. Bayes-Genis, Proteomics, 2019, 19, e1800397.

65 K. W. Witwer, B. W. M. Van Balkom, S. Bruno, A. Choo, M. Dominici, M. Gimona, A. F. Hill, D. De Kleijn, M. Koh, R. C. Lai, S. A. Mitsialis, L. A. Ortiz, E. Rohde, T. Asada, W. S. Toh, D. J. Weiss, L. Zheng, B. Giebel and S. K. Lim, J Extracell Vesicles, 2019, 8, 1609206.

66 B. Claridge, J. Lozano, Q. H. Poh and D. W. Greening, Frontiers in Cell and Developmental Biology.